Catalysis Communications 46 (2014) 36–40

Contents lists available at ScienceDirect

Catalysis Communications

journal homepage: www.elsevier.com/locate/catcom

Short Communication

Spatial confinement effects of cage-type SAPO molecular sieves on product distribution and coke formation in methanol-to-olefin reaction

Jingrun Chen [a,b], Jinzhe Li [a], Yingxu Wei [a], Cuiyu Yuan [a,b], Bing Li [a,b], Shutao Xu [a], You Zhou [a,b], Jinbang Wang [a], Mozhi Zhang [a,b], Zhongmin Liu [a,*]

[a] National Engineering Laboratory for Methanol to Olefins, Dalian National Laboratory for Clean Energy, Dalian Institute of Chemical Physics, Chinese Academy of Sciences, Dalian 116023, PR China
[b] University of Chinese Academy of Sciences, Beijing 100049, PR China

ARTICLE INFO

Article history:
Received 22 July 2013
Received in revised form 16 October 2013
Accepted 18 November 2013
Available online 23 November 2013

Keywords:
Methanol to olefin
Silicoaluminophosphate
Deactivation
Adamantane hydrocarbons
Spatial confinement

ABSTRACT

Three kinds of 8-membered ring silicoaluminophosphate (SAPO) molecular sieves with different cage structures, SAPO-34, SAPO-18 and SAPO-35, were employed in methanol-to-olefin (MTO) reaction. The main products over SAPO-34 and SAPO-18 were propene and butenes, whereas ethene and propene especially ethene were predominantly generated over SAPO-35. Coke species formation greatly depended on reaction temperature and varied systematically with cage size. The differences in production distribution and generated coke species in the MTO reaction suggest great spatial confinement effects imposed by cage structure of SAPO catalysts.

1. Introduction

The application of coal-to-olefin technology opens a new era for the production of light olefins, the backbone feedstock of petrochemical industry, from non-oil resources. Methanol-to-olefin (MTO) process has been proved to be completely successful in China [1]. Extremely high selectivity of light olefins has been obtained using a silicoaluminophosphate molecular sieve SAPO-34 with 8-membered ring pore opening and CHA supercages [2].

The mechanism of MTO reaction over microporous solid acid catalysts was extensively reported in several reviews published recently [1,3–5]. The hydrocarbon pool (HP) mechanism, supported by experimental and theoretical results [6–11], has been widely accepted. According to this mechanism with methanol conversion to hydrocarbon in an indirect way, methanol is continuously added on the "HP species" retained in the catalyst and light olefins are split off from these species. Polymethylbenzenes [6,7] and polymethylnaphthalenes [12,13] have been proposed to be the main HP species over SAPO-34. These observations indicate that the occurrence of MTO reaction following the HP mechanism requires wide space as the catalytic environment for the accommodation of bulky intermediates [10]. Recently, Bhawe and coworkers studied effect of cage size on the MTO reaction over LEV, CHA and AFX type zeolite with eight-membered ring, and they found that selectivity to ethene decreases as the cage size increases [14]. Using a first-principle kinetic study, Wispelaere and co-workers found a low-barrier path for olefin formation based on the side-chain mechanism during the MTO conversion over SAPO-34 [15].

According to the HP mechanism, MTO reaction goes through an induction period, during which HP species are formed and the fresh catalysts are transformed into working catalysts [16,17]. The further growth and aging of these active intermediates to confined coke species like polycyclic aromatics might cause the catalyst deactivation [13]. In our recent study, a new kind of non-aromatic hydrocarbon residues was found as deactivating species during the MTO reaction at low reaction temperature [18]. At reaction temperature of 300–325 °C, diamondoid hydrocarbons especially methyl-substituted adamantanes were generated as retained compounds in the nanocages of SAPO-34 and resulted in rapid deactivation [18]. Formation and accommodation of aromatics or adamantane hydrocarbons as the confined coke species, demonstrate that cage structure may provide catalytic environment for the generation of retained hydrocarbons with multiple rings.

In this contribution, three kinds of 8-membered ring cage-type SAPO molecular sieves, SAPO-34, SAPO-18 and SAPO-35, with similar physicochemical properties and close medium-strong acidity, were prepared and applied in the MTO reaction at various reaction temperatures. Based on the comparative studies, spatial confinement effects of cage structures on the production distribution and coke formation were highlighted.

* Corresponding author. Tel./fax: +86 411 84379335.
E-mail address: liuzm@dicp.ac.cn (Z. Liu).

1566-7367/$ – see front matter © 2013 Elsevier B.V. All rights reserved.
http://dx.doi.org/10.1016/j.catcom.2013.11.016

2. Experimental

2.1. Synthesis

Detailed procedure was described in Supplementary data.

2.2. Characterization

The characterization of SAPO-34, SAPO-18 and SAPO-35 using multiple techniques, including X-ray diffraction (XRD), X-ray fluorescence (XRF), scanning electron microscopy (SEM), N_2 adsorption and 2-^{13}C-acetone adsorption experiment, was described in detail in Supplementary data.

2.3. Catalytic test

Methanol conversion was performed in a fixed-bed quartz tubular reactor at atmospheric pressure. A catalyst sample of 100 mg was loaded into the reactor and the reactions were carried out at 300 °C, 350 °C and 400 °C. The methanol was fed by passing helium through a saturation evaporator with a WHSV of 2.0 h^{-1}. The reaction products were analyzed by on-line gas chromatography (Agilent GC 7890A) equipped with a HP-PLOT Q capillary column and a FID detector.

2.4. Confined organics analysis

Organic species trapped in the cages of the SAPO molecular sieves during the reaction were analyzed following the procedures as described in the literature [19]. The spent catalysts were dissolved in 20% hydrofluoric acid solution. The organic phase was extracted by dichloromethane (CH_2Cl_2), and then analyzed using an Agilent 7890A/5975C GC/MSD.

3. Results and discussion

3.1. Textural structure of silicoaluminophosphate catalysts

SAPO-34, SAPO-18 and SAPO-35 are three kinds of silicoaluminophosphate molecular sieve with 8-membered ring pore openings and different cage structures (Fig. 1). SAPO-34 possesses large CHA cages which are made up of 12 four-membered rings, 2 six-membered rings, and 6 eight-membered rings, and these cages are interconnected to six adjacent cages by 8-membered rings with pore opening of 3.8 × 3.8 Å in diameter and cage dimension of 1.27 nm × 0.94 nm. The pear-like supercages of SAPO-18 with cage dimension of 1.27 nm × 1.16 nm are also made up of analogous rings to SAPO-34, and the window dimension of AEI cages in SAPO-18 is very close to that of CHA cages in SAPO-34. The LEV cages in SAPO-35 are built from 9 four-membered rings, 5 six-membered rings, and 3 eight-membered rings, and 8-membered ring pore has a free diameter of 3.8 × 4.8 Å. Even with the window a bit of bigger than that of SAPO-34 and SAPO-18, the LEV cages in SAPO-35 with cage dimension of 0.73 nm × 0.63 nm are significantly smaller than the CHA and AEI cages.

3.2. Characterization of silicoaluminophosphate catalysts

The powder XRD patterns of calcined SAPO-34, SAPO-18 and SAPO-35 samples are shown in Fig. S1. Silicon content, crystallize size, morphology and BET surface area of prepared SAPO catalysts are shown in Table 1. The scanning electron microscope (SEM) images are shown in Fig. S2, which show that subtle differences exist in morphology and crystal size between as-synthesized samples. 2-^{13}C-acetone adsorption experiment showed that three SAPO catalysts have close medium-strong acidity.

For the effect of acidity variation with the chemical composition of the three SAPO catalysts, strong acid strength and higher acid site density will lead to more rapid catalyst deactivation due to the severe hydrogen transfer reaction [1]. In the present work, 2-^{13}C-acetone adsorption NMR experiment indicates that three SAPO catalysts employed in this study have similar moderate acid strength. XRF characterization (Table S2) shows that average Si atoms per cage in SAPO-34, SAPO-18 and SAPO-35 are 0.74, 0.70 and 1.55 separately, so acid site density is approximately close for SAPO-34 and SAPO-18, while this value is relatively higher for SAPO-35 owing to its high Si content. Recently, E. Sastre and co-workers [20] also found that MTO reaction over SAPO-34 catalysts with different silicon contents exhibits similar product distribution. Moreover, acidity amount was not considered to be the main cause of the selectivity to light olefins in the MTO reaction over cage-type small-pore molecular sieves [21].

In some previous literatures regarding MTO reaction performed over the catalysts with different crystal sizes, the selectivity to different olefins was observed to be not relevant to the crystal size of SAPO-34 [22]. G. Seo and co-workers [23] found that product compositions of MTO reactions over three SAPO-34 catalysts with different crystallite sizes were essentially the same, indicating that the mechanism of MTO reaction through polymethylbenzenes as reactive intermediates was not affected by the crystallite size of the SAPO-34 catalysts. Therefore, spatial confinement effects of the three SAPO catalysts with different cage structures may play a more important role in the product distribution.

Our recent work [24] studied the confined coke formation in the MTO reaction over the SAPO-34 catalysts with different crystal sizes, ranging from 20 nm to 8000 nm. It was found that nanosized catalysts exhibited the longest catalyst lifetime and lowest coking rate in MTO reactions, and it is worthy to note that for both of the two SAPO-34 catalysts in micrometer scale (1 μm and 8 μm), the coke species and coke amount after deactivation are very similar [24]. In the present study, the SEM images of three SAPO catalysts showed that the crystallite sizes of SAPO-34, SAPO-18 and SAPO-35 are 4–6 μm, 0.5–1 μm and 2–4 μm separately (Table 1). The subtle difference in crystallite size of three SAPO catalysts indicates that the differences in product distribution

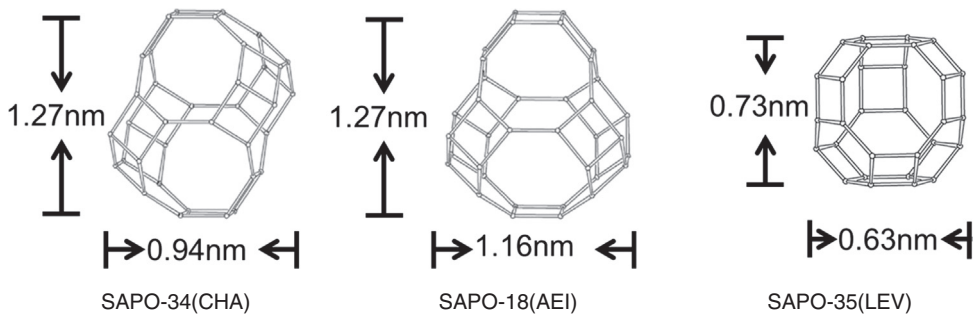

Fig. 1. Cage structure of SAPO-34, SAPO-18 and SAPO-35.

Table 1
Characterization data of 8-membered ring cage-type silicoaluminophosphate molecular sieves employed in this study.

Catalyst	Si contents in the product (mol%)[a]	Crystallize morphology and average size (μm)[b]	BET surface area[c] ($m^2\ g^{-1}$)
SAPO-34 (CHA)	6.14	Cuboids, 4–6	452.8
SAPO-18 (AEI)	5.86	Sheet, 0.5–1	477.3
SAPO-35 (LEV)	17.26	Cuboids, 2–4	521.2

[a] Determined by an X-ray fluorescence (XRF) spectrometer.
[b] Determined from scanning electron microscope (SEM) images.
[c] Determined from N_2 adsorption data.

and coke formation are more possibly caused by the spatial confinement effects of different cages in the three SAPO catalysts.

Considering similar physico-chemical properties and close medium-strong acidity of SAPO catalysts employed in the present work, a comparative study of MTO reaction was conducted over SAPO-34, SAPO-18 and SAPO-35 with different cage structures, to highlight the spatial confinement effects of cage structure on the product distribution and coke formation.

3.3. Spatial confinement effects on the product distribution of MTO conversion

The product distribution of MTO reaction over SAPO catalysts at different reaction temperatures is shown in Fig. 2. When MTO reaction was performed at 300 °C and 350 °C, propene and butenes were predominantly formed over SAPO-18 and SAPO-34, while ethene and propene especially ethene were generated as the main products over SAPO-35 under the same condition, corresponding to the LEV cage with the smallest size among the three SAPO catalysts. At 400 °C, enhanced reaction temperature improved ethene selectivity while depressed the production of butenes and higher hydrocarbons. It should still be mentioned that butene formation is more prominent over SAPO-18 than SAPO-34, possibly stemming from the slightly larger space provided by pear-like AEI cages of SAPO-18 compared with the CHA cages of SAPO-34.

Analysis of confined organics (Fig. S6) retained in cages of SAPO catalysts formed during the initial reaction period (TOS = 15 min) at 300 °C indicated that tetramethylbenzene, pentamethylbenzene and hexamethylbenzene were predominantly formed over SAPO-34 and SAPO-18, but trimethylbenzene, tetramethylbenzene and pentamethylbenzene were dominating species over SAPO-35. Haw and co-workers [8] discovered that the formation of confined polymethylbenzenes influenced the olefin product distribution. Tetra-, penta- and hexamethylbenzene formation is favorable for propene generation but xylene and trimethylbenzene formation leads predominantly to ethene production, indicating that product distribution is strongly influenced by the number of methyl groups on confined polymethylbenzenes. The above results exhibited steric limitations of LEV cages on polymethylbenzene formation and can also be used to explain the predominant production of ethene over SAPO-35.

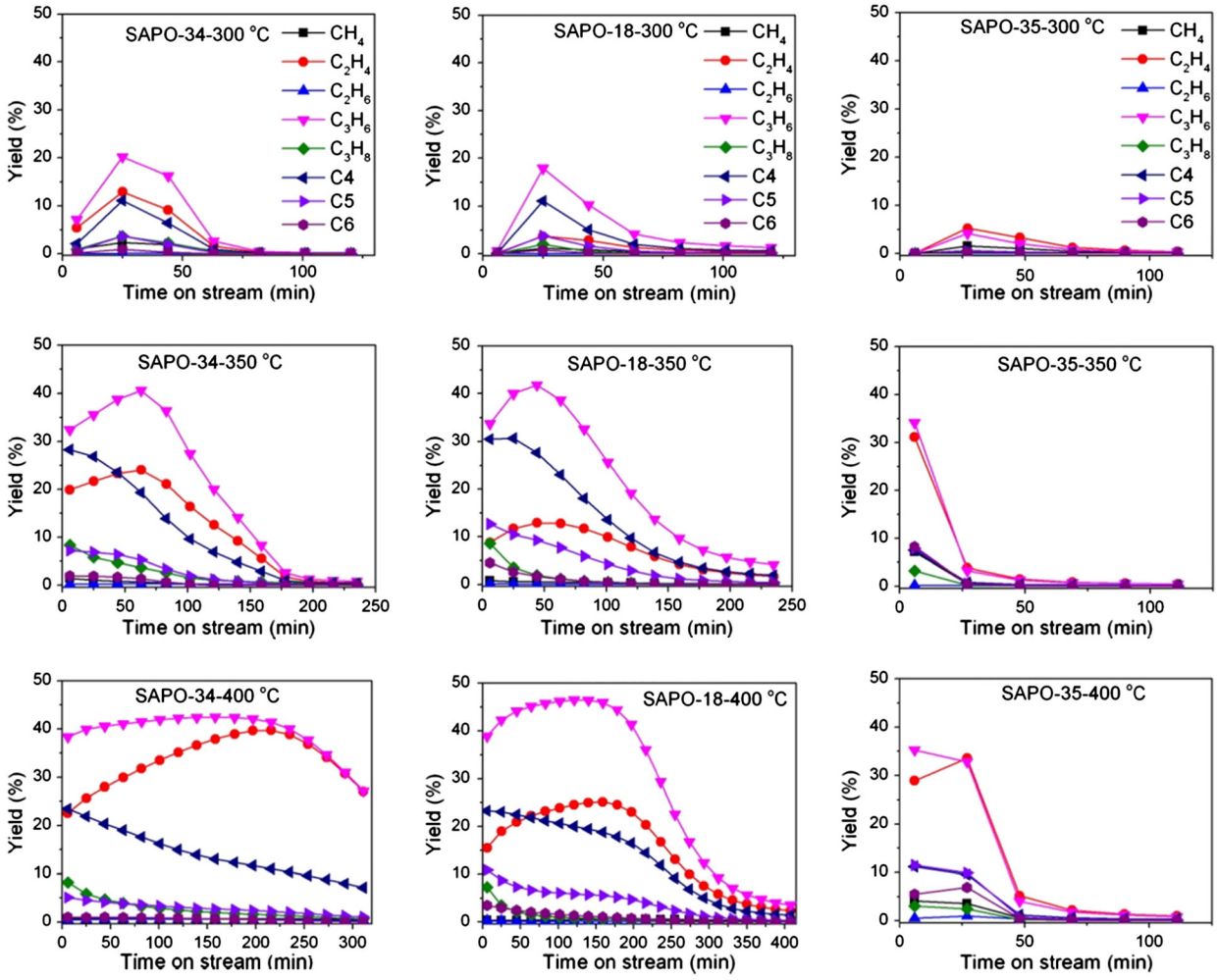

Fig. 2. Product distribution of MTO reaction over SAPO-34, SAPO-18 and SAPO-35 at various reaction temperatures (300 °C, 350 °C and 400 °C).

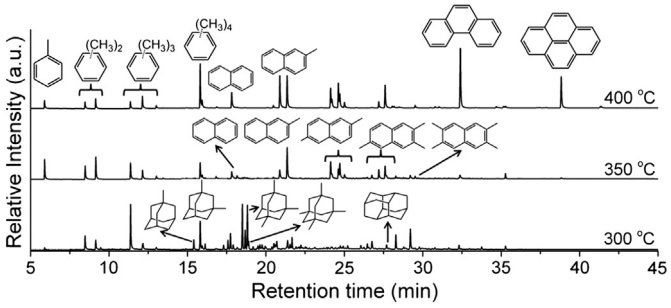

Fig. 3. GC–MS chromatograms of the hydrocarbon compounds retained in the deactivated SAPO-34 catalyst at various temperatures.

Cage structure of SAPO molecular sieves is of utmost importance for the formation of HP species, resulting in a strong structural dependence of product distribution.

3.4. Spatial confinement effects of cage structure on coke formation

3.4.1. Coke species determination of the deactivated SAPO catalysts

The compositions of the organic materials retained in the deactivated SAPO-34 catalyst at various temperatures are described in detail in Fig. 3. Hydrogen-unsaturated coke species tended to be formed at relatively high temperature. At 400 °C, the formation of polycyclic aromatic hydrocarbons such as phenanthrene and pyrene was responsible for catalyst deactivation. At 350 °C, most coke species were polymethylnaphthalenes. Uniquely, the formation of adamantane hydrocarbons in the CHA cages of SAPO-34 accounted for the rapid deactivation at 300 °C [18].

Aromatics and adamantane hydrocarbons were also observed among the coke species of the deactivated catalysts over SAPO-18 and SAPO-35. And interestingly, the confined organic distribution was closely correlated with cage structure of the SAPO catalysts and reaction temperature. More detailed discussions about coke species and the correlation of these confined organics with cage structure are presented in the next section.

Since coke species retained in the catalyst varied with reaction temperature, reaction conditions under which aromatics or adamantane hydrocarbons were favored to be generated should be considered in the study of MTO reaction over the SAPO molecular sieves. The relative distribution of adamantane species and aromatic compounds retained in deactivated SAPO-34, SAPO-18 and SAPO-35 catalysts at different temperatures is shown in Fig. S7. At 300 °C, retained materials over all the SAPO molecular sieves were dominated by adamantane species, but the proportion of aromatic compounds grows rapidly with temperature increase. At 350 °C, only a small amount of adamantane species could be detected. At 400 °C, retained hydrocarbons in the cages of the deactivated SAPO-34 and SAPO-18 catalysts were almost aromatic compounds, and only trace amount of adamantane species can be found in cages of the deactivated SAPO-35 catalyst.

3.4.2. Spatial confinement effects on the coke formation

When the reaction temperature was higher than 350 °C, aromatic compounds appeared as the main retained materials, and the bulky polycyclic aromatics caused the catalyst deactivation. Confined aromatic compounds in the deactivated catalysts varied with the cage structure of SAPO catalysts. Relative distribution of these aromatic compounds among the confined organics in the deactivated SAPO-34, SAPO-18 and SAPO-35 catalysts is shown in Fig. 4. At 400 °C, monocyclic and bicyclic aromatic compounds appeared among the confined coke species in the three deactivated catalysts, but polycyclic aromatic compounds can only be detected in the deactivated SAPO-34 and SAPO-18. These results implied that the LEV cages of SAPO-35 sterically inhibit the formation of large aromatic organics, while the cages of SAPO-34 and SAPO-18 provide enough space for the accommodation of polycyclic aromatic compounds. At 350 °C, most aromatic compounds were monocyclic and bicyclic, and only a small amount of polycyclic aromatic compounds was found in the deactivated SAPO-34. At 300 °C, all the aromatic compounds were monocyclic.

Adamantane hydrocarbons are predominant at 300 °C, so detailed analysis has also been performed to clarify the spatial confinement effects imposed by the cage structure on the formation of adamantane hydrocarbons in the deactivated SAPO-34, SAPO-18 and SAPO-35 catalysts. As shown in Fig. 5, in the deactivated SAPO-34 catalyst, dimethyladamantane (DMA) and trimethyladamantane (TMA) were the main retained organics with nearly the same proportion. Moreover, considerable amounts of tetramethyladamantane (TeMA), small portion of methyladamantane (MA), as well as trace of adamantane (A) were also detected. For the deactivated SAPO-18 catalyst, the order of adamantane hydrocarbon amount was TMA > DMA ≈ TeMA > MA > A. However, for the deactivated SAPO-35 catalyst, only A, MA and a small amount of DMA appeared among the retained adamantane hydrocarbons.

The significant differences among distributions of the coke species confined in the cages of the three deactivated SAPO catalysts could be correlated well with the cage structure variation. Large-size cages of SAPO-34 and SAPO-18 favored the formation of polycyclic aromatic compounds and poly-methyl-substituted adamantanes. Subtle differences between cage structure of SAPO-34 and SAPO-18 cause slight variation of the relative proportion of the cyclic aromatics as well as the distribution of poly-methyl-substituted adamantanes. However, the cages of SAPO-35 with the smallest cage size spatially inhibited the formation of polycyclic aromatics involving pyrene and phenanthrene, and large adamantane hydrocarbons such as DMA, TMA and TeMA, yet favored the formation of aromatic and adamantane hydrocarbons with smaller size.

4. Conclusion

MTO conversion was performed over three cage-type SAPO molecular sieves with narrow pore opening. Varied product distribution over different SAPO catalysts was closely related with the formation of

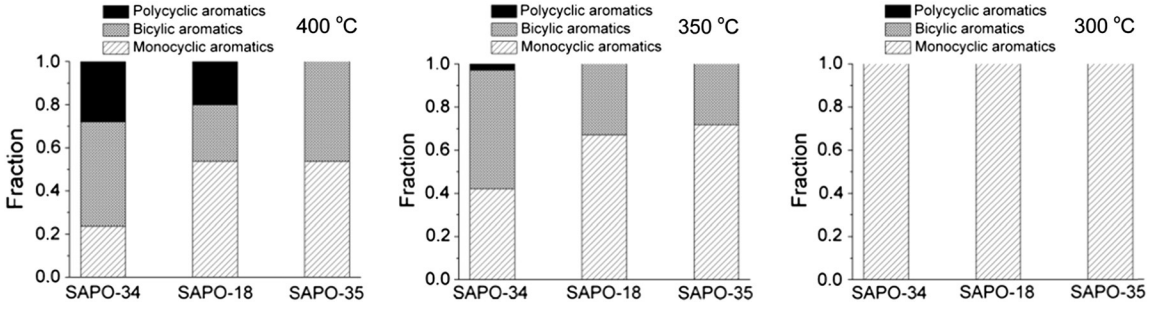

Fig. 4. Relative distribution of monocyclic, bicyclic and polycyclic aromatic compounds in the deactivated SAPO-34, SAPO-18 and SAPO-35 catalysts at 400 °C (left panel), 350 °C (middle panel) and 300 °C (right panel).

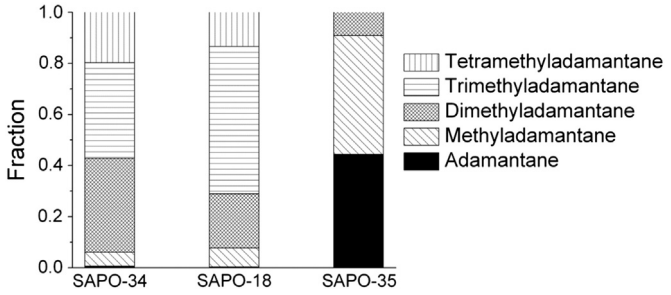

Fig. 5. Relative distribution of adamantane hydrocarbons in the deactivated SAPO-34, SAPO-18 and SAPO-35 catalysts at 300 °C.

reactive polymethylbenzene intermediates as HP species retained in different cage structures. Coke species generation greatly depended on reaction temperature. Different from the deactivation at high reaction temperature with polycyclic aromatics as the coke species, deactivation of cage-type SAPO catalysts at 300 °C originated from the formation of adamantane hydrocarbons confined in the catalyst. Even though the deactivation mode differed at low and high reaction temperatures, generation of aromatics and adamantane hydrocarbons as coke species both reflected spatial confinement effects imposed by the cage structure of SAPO molecular sieves.

Acknowledgement

The authors thank the financial support from the National Natural Science Foundation of China (Nos. 21273005, 21273230 and 21103180).

Appendix A. Supplementary data

Supplementary data to this article can be found online at http://dx.doi.org/10.1016/j.catcom.2013.11.016.

References

[1] U. Olsbye, S. Svelle, M. Bjorgen, P. Beato, T.V.W. Janssens, F. Joensen, S. Bordiga, K.P. Lillerud, Angew. Chem. Int. Ed. 51 (2012) 5810–5831.
[2] J. Liang, H.Y. Li, S. Zhao, W.G. Guo, R.H. Wang, M.L. Ying, Appl. Catal. 64 (1990) 31–40.
[3] D. Chen, K. Moljord, A. Holmen, Microporous Mesoporous Mater. 164 (2012) 239–250.
[4] K. Hemelsoet, J.V.d. Mynsbrugge, K.D. Wispelaere, M. Waroquier, V. Van Speybroeck, ChemPhysChem 14 (2013) 1526–1545.
[5] S. Ilias, A. Bhan, ACS Catal. 3 (2013) 18–31.
[6] W.G. Song, J.F. Haw, J.B. Nicholas, C.S. Heneghan, J. Am. Chem. Soc. 122 (2000) 10726–10727.
[7] B. Arstad, S. Kolboe, J. Am. Chem. Soc. 123 (2001) 8137–8138.
[8] W.G. Song, H. Fu, J.F. Haw, J. Am. Chem. Soc. 123 (2001) 4749–4754.
[9] S. Svelle, F. Joensen, J. Nerlov, U. Olsbye, K.P. Lillerud, S. Kolboe, M. Bjorgen, J. Am. Chem. Soc. 128 (2006) 14770–14771.
[10] D. Lesthaeghe, B. De Sterck, V. Van Speybroeck, G.B. Marin, M. Waroquier, Angew. Chem. Int. Ed. 46 (2007) 1311–1314.
[11] D.M. McCann, D. Lesthaeghe, P.W. Kletnieks, D.R. Guenther, M.J. Hayman, V. Van Speybroeck, M. Waroquier, J.F. Haw, Angew. Chem. Int. Ed. 47 (2008) 5179–5182.
[12] W.G. Song, H. Fu, J.F. Haw, J. Phys. Chem. B 105 (2001) 12839–12843.
[13] M. Bjorgen, U. Olsbye, S. Kolboe, J. Catal. 215 (2003) 30–44.
[14] Y. Bhawe, M. Moliner-Marin, J.D. Lunn, Y. Liu, A. Malek, M. Davis, ACS Catal. 2 (2012) 2490–2495.
[15] K. De Wispelaere, K. Hemelsoet, M. Waroquier, V. Van Speybroeck, J. Catal. 305 (2013) 76–80.
[16] J.F. Haw, W.G. Song, D.M. Marcus, J.B. Nicholas, Acc. Chem. Res. 36 (2003) 317–326.
[17] W. Wang, A. Buchholz, M. Seiler, M. Hunger, J. Am. Chem. Soc. 125 (2003) 15260–15267.
[18] Y.X. Wei, J.Z. Li, C.Y. Yuan, S.T. Xu, Y. Zhou, J.R. Chen, Q.Y. Wang, Q. Zhang, Z.M. Liu, Chem. Commun. 48 (2012) 3082–3084.
[19] M. Guisnet, L. Costa, F.R. Ribeiro, J. Mol. Catal. A Chem. 305 (2009) 69–83.
[20] T. Alvaro-Munoz, C. Marquez-Alvarez, E. Sastre, Catal. Today 213 (2013) 219–225.
[21] Q.J. Zhu, J.N. Kondo, R. Ohnuma, Y. Kubota, M. Yamaguchi, T. Tatsumi, Microporous Mesoporous Mater. 112 (2008) 153–161.
[22] D. Chen, K. Moljord, T. Fuglerud, A. Holmen, Microporous Mesoporous Mater. 29 (1999) 191–203.
[23] K.Y. Lee, H.J. Chae, S.Y. Jeong, G. Seo, Appl. Catal. A Gen. 369 (2009) 60–66.
[24] G.J. Yang, Y.X. Wei, S.T. Xu, J.R. Chen, J.Z. Li, Z.M. Li, J.H. Yu, R.R. Xu, J. Phys. Chem. C 117 (2013) 8214–8222.